

Phase transition in two-dimensional dipolar fluids at low densities

J. M. Tavares,^{1,2} J. J. Weis,³ and M. M. Telo da Gama¹

¹*Centro de Física Teórica e Computacional da Universidade de Lisboa, Avenida Professor Gama Pinto 2, P-1649-003 Lisboa, Portugal*

²*Instituto Superior de Engenharia de Lisboa, Rua Conselheiro Emídio Navarro, 1, P-1949-014 Lisboa, Portugal*

³*Laboratoire de Physique Théorique, Université de Paris XI, Bâtiment 210, F-91405, Orsay Cedex, France*

(Received 2 May 2005; revised manuscript received 24 January 2006; published 17 April 2006)

Monte Carlo computer simulations of a quasi two-dimensional (2D) dipolar fluid at low and intermediate densities indicate that the structure of the fluid is well described by an ideal mixture of self-assembling clusters. A detailed analysis of the topology of the clusters, of their internal energy and of their size (or mass) distributions is used to obtain approximations to their partition functions. Within the scope of these approximations, the results of this work suggest that the 2D dipolar fluid undergoes a phase transition from a dilute phase characterized by a number of disconnected clusters to a condensed phase characterized by a network or spanning (macroscopic) cluster that includes most of the particles in the system.

DOI: 10.1103/PhysRevE.73.041507

PACS number(s): 61.20.Ja, 61.20.Gy, 75.50.Mm, 68.65.-k

I. INTRODUCTION

The condensation of simple fluids results from the free energy balance of the high entropy gas and the low energy liquid phases. This transition appears to be generic in simple fluids interacting through isotropic intermolecular potentials that are repulsive at short distances and attractive otherwise. The dipolar hard sphere (DHS) fluid is a model where hard (or soft) spheres with an embedded central dipole interact through the dipole-dipole potential. As the average dipolar interaction between two dipoles (weighted by the Boltzmann factor) is attractive one may anticipate phase behavior analogous to that of simple fluids. Indeed, a recent calculation of the free energy of the DHS at several temperatures, based on Monte Carlo (MC) simulations [1], suggests the presence of an isotropic fluid-fluid transition at low densities, lending some support to the analogy with simple fluids. However, the structure of DHS at low densities, where the transition has been reported, is drastically different from that of isotropic fluids. Numerical simulations of DHS [2] (and also of Stockmayer fluids [3]) for dipolar interaction strengths of the order of the thermal energy, have shown that the anisotropy of the dipolar potential promotes the formation of self-assembled aggregates (chains, rings and more complex clusters—see Fig. 1) in sharp contrast with the isotropic compact clusters observed in simple fluids. Moreover, the pair correlation function of DHS is strongly peaked at contact and the internal energy is nearly independent of the density at odds with the behavior of simple fluids.

Association theories [4–8], that include the effect of cluster formation in the thermodynamics, describe rather well the slow variation of the internal energy with the density and the size (or mass) distribution of the clusters. The simplest of these theoretical approaches (based on simulation results [2,6,8]) assumes that the only effect of the dipolar interaction is to drive cluster formation and in this setting the DHS is described as an ideal mixture of self-assembling clusters. These theories fail to predict the existence of phase transitions unless interactions among the clusters are added.

In a recent paper [8] we have found that various types of clusters are formed in a quasi two-dimensional (2D) DHS fluid (cf. Fig. 1): chains, rings and defect clusters (renamed

networks in what follows as in [9,10]). The dipolar chains and rings at very low densities were fully characterized by analyzing their conformational properties, internal energy and size (or mass) distribution, and a strong analogy with equilibrium polymers [11] was found. However, we did not address the question of the phase transition due to the difficulty in extending the analysis to networks for the low density systems that were simulated [8]. In order to overcome these problems we have performed longer simulations at higher densities (along one isotherm only) and found a way of including the effect of network formation in an association theory of ideal self-assembly. This has allowed us to conclude that the simulation results suggest the presence of a phase transition in the quasi 2D DHS.

We note that understanding the nature of this phase transition is important for applications based on dispersions of ferromagnetic nanoparticles [12,13], where strong dipolar interactions are present, as well as for theoretical reasons. In fact, the interplay between cluster formation and condensation is a general problem, relevant in a variety of other theoretical contexts [10].

This paper is organized as follows. In Sec. II, the details of MC simulations and the analysis of the structure of the fluid are presented. In Sec. III we describe (following [14]) how a phase transition may occur in an ideal self-assembling system and how networks can be included in the theory. Finally, in Sec. IV we combine the results of Secs. II and III to verify that the results of simulations of the quasi 2D DHS indicate the existence of a phase transition.

II. MONTE CARLO SIMULATIONS AND THE STRUCTURE OF THE QUASI 2D DHS FLUID

We have performed extensive MC simulations in the canonical ensemble for systems of hard spheres with diameter σ and dipole strength m , interacting through the pair potential

$$U_{\text{DHS}} = U_{\text{HS}} - \frac{m^2}{r_{12}^3} [3(\hat{\mu}_1 \cdot \hat{r}_{12})(\hat{\mu}_2 \cdot \hat{r}_{12}) - \hat{\mu}_1 \cdot \hat{\mu}_2]. \quad (1)$$

The term r_{12} is the distance between spheres 1 and 2, U_{HS} the hard-sphere potential ($=\infty$ if $r_{12} < \sigma$, 0 otherwise), $\hat{r}_{12} \equiv \frac{\vec{r}_2 - \vec{r}_1}{r_{12}}$

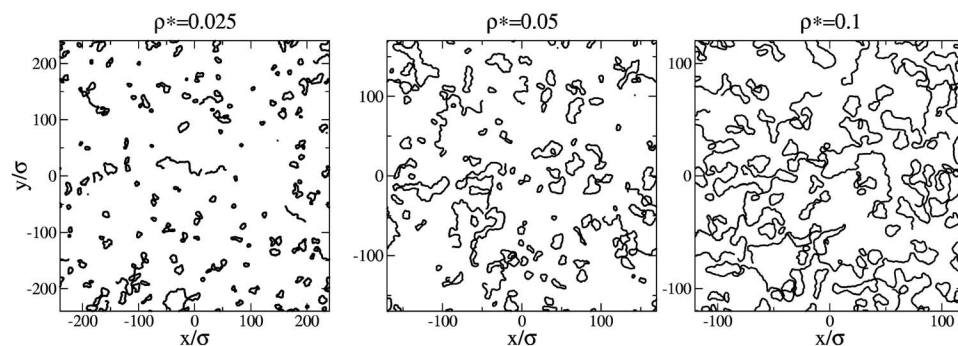


FIG. 1. Typical equilibrium configurations of the quasi 2D DHS as obtained from MC simulations with $N_p=5776$ at $m^*=2.75$ and three reduced densities.

the unit interparticle vector and $\hat{\mu}_1, \hat{\mu}_2$ the unit vectors in the direction of the dipole moments of spheres 1 and 2, respectively. The centers of the spheres and their dipole moments were constrained to lie on the same plane, and thus the model is a quasi 2D dipolar hard sphere fluid [8].

We used $N_p=5776$ particles in a square box with periodic boundary conditions and, for the isotherm $m^* \equiv m(\sigma^3 k_B T)^{-1/2} = 2.75$, simulations were performed as described in [8], at reduced densities $\rho^* \equiv \sigma^2 N_p / A = 0.05, 0.0625, 0., 0.075, 0.1, 0.15$ and 0.2 (A is the area of the simulation box). An appropriate Ewald sum [8,15], which in 2D is absolutely convergent, was used to account for the long range of the dipolar interaction. As at the dipole moment and range of densities considered the dipolar spheres have a strong tendency for clustering (see below) MC trial moves involved both single particle moves (translation and rotation) as well as cluster moves (translation of a whole cluster).

Calculations at different densities were started from an initial configuration with no clusters and of the order of 5×10^6 cycles (i.e., attempts to rotate and move each of the N_p dipolar spheres) were discarded to allow for equilibration. Between 100 (low densities) and 400 (high densities) configurations were generated for analysis of the equilibrated system. For each density, the configurations were obtained from three independent runs and, in each run, the configurations were separated by $\approx 1,5 \times 10^5$ MC cycles. Analysis of the autocorrelation function of the internal energy indicates a correlation time of about 10^6 MC cycles. By comparison to the simulations performed at lower densities and for the same m^* and N_p in [8], the number of MC cycles is larger by a factor of 2–6.

Figure 1 shows snapshots of equilibrium configurations and evidence that the structure of this system is nontrivial. The particles tend to aggregate in clusters of several sizes and topologies; some clusters exhibit linear aggregation only (chains and rings) and all of the others (networks) have branches even if most of their particles are still linearly aggregated. This qualitative picture is quantified [8] by defining a circle of diameter r_c around each particle i : if there are one, two or more additional particles within this circle, then i is an end, an interior or a junction particle, respectively [10]. Two particles belong to a given cluster if their separation is less than r_c and the topology of a cluster is determined by the number of ends and junctions: rings have interior particles only, chains have two ends and no junctions, and networks have at least one junction. The cutoff r_c must be $\approx \sigma$ and in this work we took $r_c = 1.15\sigma$.

Both the total internal energy of the system and the internal energy of the clusters decrease $\approx 0.5\%$ when the density is increased from $\rho^* = 0.025$ to 0.1 . At all densities, the difference between these two energies is of the order of 0.5% , and well defined size distributions are observed even though the clusters break and recombine during a simulation run. Thus, as in previous works [4–8], the description of the system as an ideal mixture of self-assembling clusters is justified.

In order to characterize the structure of the quasi 2D DHS we have calculated, for each density, the size distribution of chains, rings and networks, i.e., the mean number of clusters of each topology with N particles. In Fig. 2 we plot the results obtained for $\rho^* = 0.1$ (notice that we use histograms of bin size ≈ 20 , which is roughly half of the mean chain length at $m^* = 2.75$ —see [8]). Similar results are obtained down to $\rho^* = 0.05$. The thick lines are the theoretical predictions for the chain and ring length distributions obtained in [8] by assuming that each chain and ring can be considered as a dilute ideal polymer. The agreement with the new simulation results shows that this hypothesis holds up to $\rho^* = 0.1$, giving further support to the description of the DHS as an ideal mixture of self-assembling clusters. Figure 2 also shows that the exponential decay of the network distribution for large values of N at $\rho^* = 0.1$ is smaller than that of the chain distribution. This difference is found at all densities studied (including those in [8]) and grows with increasing

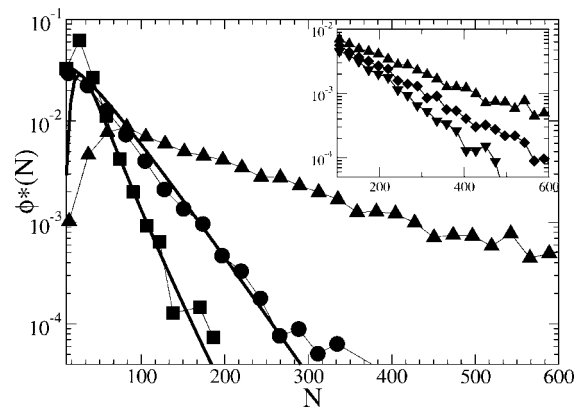


FIG. 2. Mean reduced density of chains [circles, $\phi^*(N, 2, 0)$], rings [squares, $\phi^*(N, 0, 0)$] and networks [triangles, $\phi_n^*(N)$] of size N , as obtained from simulations with $\rho^* = 0.1$. The lines are the theoretical predictions for the chains and rings. Inset: mean reduced density of networks at $\rho^* = 0.05$ (inverted triangles), $\rho^* = 0.0625$ (diamonds) and $\rho^* = 0.1$ (triangles).

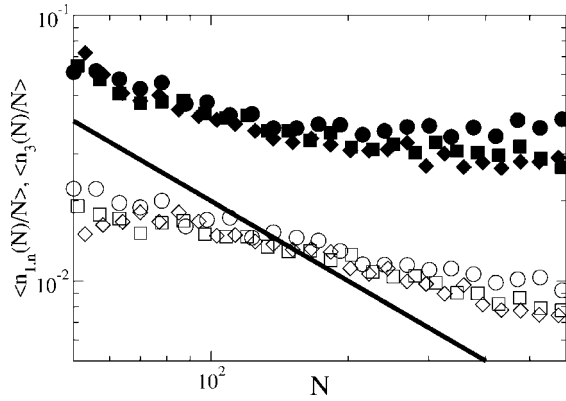


FIG. 3. Mean fraction of ends $\langle n_{1,n} \rangle / N$, open symbols) and junctions $\langle n_3 \rangle / N$, full symbols) in networks of size N , at $\rho^* = 0.1$ (circles), 0.075 (squares) and 0.0625 (diamonds). Simulation results are for clusters with N in the range 50–600. The statistical uncertainty of these results is of the order of the size of the symbols. The full line is the function $2/N$, the fraction of ends in chains of size N .

density. This growth is due mainly to the decreasing decay of the network distribution with increasing density, as depicted in the inset of Fig. 2.

As mentioned previously, networks are defined as clusters with at least one junction. This means that, by contrast to chains and rings, the number of junctions and ends of a network of length N is not defined *a priori*. To characterize the typical topology of networks we have calculated the mean number of ends, $\langle n_{1,n}(N) \rangle$, and of junctions, $\langle n_3(N) \rangle$, at densities $\rho^* = 0.0625, 0.075$ and 0.1 , for networks of length N . The result of this calculation is shown in Fig. 3. For the sake of comparison, we have plotted in the same figure $2/N$, i.e., the fraction of ends in chains of length N . For every density, both $\langle n_{1,n}(N) \rangle / N$ and $\langle n_3(N) \rangle / N$ are decreasing functions of N that decay slower than N^{-1} . For large N (most notably for $\rho^* = 0.1$) $\langle n_3(N) \rangle / N$ appears to reach (within the statistical error) a constant value that increases slightly as the density increases.

Figures 2 and 3 show results for $\rho^* \leq 0.1$ only. In fact, in simulations with $\rho^* = 0.15$ and 0.2 we have observed very strong finite size effects. The distribution $\phi_n(N)$ does not decay exponentially for large N since, in most of the configurations analyzed, around 5000 particles belong to the same network. This is an expected finite size effect: since the particles self-assemble in larger aggregates as the density increases (see [8]), for any finite system there is a density above which all the particles will belong to the same network. Given that this density is, for the system under study, larger than $\rho^* = 0.1$, for $\rho^* \leq 0.1$ these finite size effects are negligible. As a consequence we will assume that the trends shown in Figs. 2 and 3 can be extended to much larger values of N .

The results shown in Figs. 2 and 3 also justify the choice of only one (large) value of N_p for the simulations. If smaller values of N_p were used the distributions represented in those figures would have an effective cutoff at lower values of N , and extrapolations to the large N limit (see the next sections) would be less reliable.

III. PHASE TRANSITION IN IDEAL SELF-ASSEMBLING SYSTEMS WITH CHAINS, RINGS AND NETWORKS

The Helmholtz free energy density, f , of a system of volume V (or area A in 2D), at absolute temperature T and with N_p particles that self-assemble to form noninteracting clusters of size N ($1 \leq N \leq N_p$), is [8,14]

$$\beta f = \sum_{N=1}^{N_p} \phi(N) [\ln \phi(N) - 1 - \ln q(N)], \quad (2)$$

where $\beta \equiv (k_B T)^{-1}$ (k_B is Boltzmann's constant); $\phi(N)$ and $Vq(N)$ are, respectively, the density and the partition function of clusters of size N . The free energy f is minimized with respect to the densities $\phi(N)$, subject to a normalization condition $N_p/V = \sum_{N=1}^{N_p} N\phi(N)$, yielding the set of equations [8]

$$\phi(N) = q(N) \exp[N\beta\mu(N_p, \rho)], \quad (3)$$

where $\mu(N_p, \rho)$ is the chemical potential of a system with N_p particles and density $\rho \equiv N_p/V$. In general [16], the partition function $q(N)$ may be written as

$$q(N) = F(N) \exp(-\beta\lambda N), \quad (4)$$

where λ is the free energy per particle of an infinite cluster and $-\beta^{-1} \ln[VF(N)]$ is a sublinear correction (in N) to that free energy. The substitution of Eqs. (3) and (4) in the normalization condition results in

$$\rho = \sum_{N=1}^{N_p} NF(N) \exp[\beta(\mu(N_p, \rho) - \lambda)N] \quad (5)$$

and defines implicitly $\mu(N_p, \rho)$. The phase behavior of the system is obtained from the equation of state $\mu(\rho) \equiv \lim_{N_p \rightarrow \infty} \mu(N_p, \rho)$, i.e., the thermodynamic limit of Eq. (5). This limit depends crucially on the convergence of the sum $\rho_t \equiv \sum_{N=1}^{\infty} NF(N)$ and may be obtained with the help of a generic graphical representation of $\mu(N_p, \rho)$ as given by Eq. (5) (see Fig. 4).

Let us first consider the case when ρ_t diverges. From Eq. (5) one concludes that for every value of ρ it is always possible to find a (finite) value of N_p such that $\mu(N_p, \rho) = \lambda$, and that this value increases with ρ . Therefore, one has $\mu(\rho) \equiv \lim_{N_p \rightarrow \infty} \mu(N_p, \rho) < \lambda$ and $\lim_{\rho \rightarrow \infty} \mu(\rho) = \lambda$, which leads to the schematic representation of Fig. 4(a). Consider now the case when ρ_t is finite. For every $\rho < \rho_t$ it is always possible to find a (finite) value for N_p such that $\mu(N_p, \rho) = \lambda$. This value increases when ρ approaches ρ_t so that $\mu(\rho) \equiv \lim_{N_p \rightarrow \infty} \mu(N_p, \rho) < \lambda$ and $\mu(\rho_t) = \lambda$. On the other hand, for every $\rho > \rho_t$ and every (finite) N_p one must have $\mu(N_p, \rho) > \lambda$. At the same time, for every fixed $\rho > \rho_t$ any increase in N_p entails a decrease in $\mu(N_p, \rho)$. As a consequence, when $\rho > \rho_t$, $\mu(\rho) \equiv \lim_{N_p \rightarrow \infty} \mu(N_p, \rho) = \lambda$.

Therefore, if ρ_t diverges then $\mu(\rho)$ is an analytic increasing function of ρ , bounded by λ ($\mu(\rho) < \lambda$). Consequently, when ρ_t diverges, the system does not exhibit a phase transition. On the other hand, if ρ_t is finite, $\mu(\rho)$ converges non-uniformly to the function: $\mu(N_p \equiv \infty, \rho)$ [given through Eq. (5)] if $\rho < \rho_t$; and λ if $\rho \geq \rho_t$. Then, for finite ρ_t , $\mu(\rho)$ is singular at $\rho = \rho_t$, signaling a phase transition at this density:

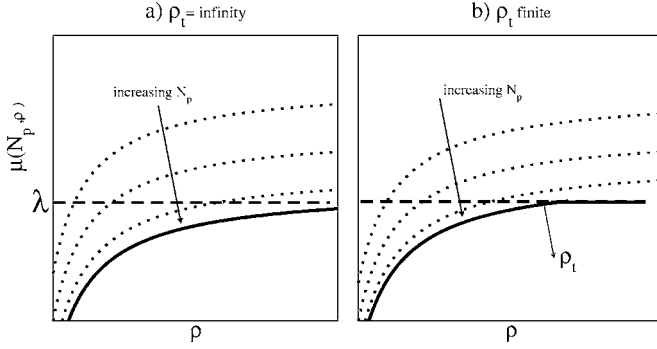


FIG. 4. General representation of the solutions of Eq. (5) for different values of N_p . Dotted lines: $\mu(N_p, \rho)$ for finite N_p . Full line: $\mu(\rho) \equiv \lim_{N_p \rightarrow \infty} \mu(N_p, \rho)$; (a) and (b) represent systems where $\rho_t \equiv \sum_{N=1}^{\infty} N \bar{F}(N)$ [see Eq. (5)] is infinite and finite, respectively. In case (b), the discontinuity in the derivative of $\mu(\rho)$ at $\rho = \rho_t$ signals the existence of a phase transition; λ (dashed line) is the free energy per particle of an infinite cluster.

when $\rho < \rho_t$ the structure consists of small disconnected clusters ($\mu(\rho) < \lambda$) and when $\rho \geq \rho_t$ any excess particles (with respect to ρ_t) condense in an “infinite,” spanning cluster ($\mu(\rho) = \lambda$).

This transition is similar to a variety of other transitions [14]—lamellae formation in systems of disk-like micelles, emulsification failure in microemulsions, Bose-Einstein condensation, etc.—where condensation is not driven by the interactions between “particles” (or aggregates).

Previous applications of association theories to the DHS considered chain and ring formation only [4,5,7,8] and failed to predict a phase transition. Indeed, infinite chains and rings have the same configurational entropy [16] and internal energy [8] per particle. Their behavior is similar to that of self-avoiding random walks with $F(N) \propto (N^{\gamma-1} + N^{-3+\alpha})$, where γ and α are universal exponents known from polymer theory [16]. Since $\gamma \geq 1$, $\rho_t \rightarrow \infty$ and the absence of a phase transition follows from Eq. (5).

In order to account for the effects of network formation, the theory entailed in Eqs. (3), (4), and (5) must be generalized to include N clusters with different topologies. To do so, we consider that each N cluster can be classified according to its number of ends, n_1 , and junctions, n_3 [8–10].

The partition function of a cluster of size N is now $Vq(N, n_1, n_3)$, with

$$q(N, n_1, n_3) = F(N, n_1, n_3) \exp[-N\beta\lambda(x_1, x_3)], \quad (6)$$

where $\lambda(x_1, x_3)$ is the free energy per particle of an infinite cluster with a fraction of ends $x_1 \equiv n_1/N$ and a fraction of junctions $x_3 \equiv n_3/N$, and $-\beta^{-1} \ln VF(N, n_1, n_3)$ is the sublinear correction to that free energy. The generalization of Eq. (3) for the density of clusters of size N with topology (n_1, n_3) is

$$\phi(N, n_1, n_3) = F(N, n_1, n_3) \exp[\beta N(\mu - \lambda(x_1, x_3))]. \quad (7)$$

The implementation of this approach requires the knowledge of $q(N, n_1, n_3)$ for networks (i.e., for $n_3 \neq 0$), and simulation results for the various cluster distribution functions.

Unfortunately, this is not possible at present, as the number of configurations of a network of N monomers, with n_1 ends and n_3 junctions, is not known and simulations do not yield reliable distribution functions for clusters with arbitrary topologies. In order to proceed, we note that an increase in the number of junctions and ends of a N cluster increases the internal energy, while it decreases the volume available to branches, decreasing the translational entropy of the network. However, the number of possible branched architectures increases, increasing the configurational entropy of the network. We may then conjecture that, at fixed N , the function $q(N, n_1, n_3)$ will exhibit a maximum for some $[\bar{n}_1(N), \bar{n}_3(N)]$. If, in the spirit of the saddle-point approximation, only this maximum is considered the mean density of networks of size N , $\phi_n(N)$, is

$$\phi_n(N) = F_n(N, \bar{n}_1, \bar{n}_3) \exp[\beta N(\mu - \lambda(\bar{x}_1, \bar{x}_3))], \quad (8)$$

where $\bar{x}_1 \equiv \bar{n}_1(N)/N$ and $\bar{x}_3 \equiv \bar{n}_3(N)/N$. Substituting this (and the corresponding expressions for chains and rings obtained in [8]) in Eq. (5) yields the equation of state. Further analysis requires the knowledge of the functions F , $\bar{n}_1(N)$ and $\bar{n}_3(N)$. In the next section we will use the simulation results of Sec. II to obtain the relevant information.

IV. PHASE TRANSITION IN THE QUASI 2D DHS

The study of the phase transition in the quasi 2D DHS reduces, in the present context and approximations, to the analysis of the thermodynamic limit of the generalization of Eq. (5) to include chains, rings and networks

$$\rho^* = \sum_{N=1}^{N_p} N [\phi_c(N, \mu) + \phi_r(N, \mu) + \phi_n(N, \mu)]. \quad (9)$$

Reliable approximations for the length distributions of chains, $\phi_c(N, \mu)$, and rings, $\phi_r(N, \mu)$, at a fixed temperature and for large N , are already known from [8]: $\phi_c(N, \mu) \propto N^{\gamma-1} \exp(\beta(\mu - \lambda_0)N)$ and $\phi_r(N, \mu) \propto N^{-3+\alpha} \exp(\beta(\mu - \lambda_0)N)$, where λ_0 is the free energy per particle of infinite chains and rings, and γ , α are universal exponents from polymer theory ($\gamma = 1.34$ and $\alpha = 0.5$ for 2D self avoiding walks [16]). If we consider that the network distribution function $\phi_n(N)$ is in general given by Eq. (8), then Eq. (9) can be rewritten as

$$\rho^* = \sum_{N=1}^{N_p} [G_{rc}(N) + G_n(N)] \times \exp\{\beta[\mu(N_p, \rho^*) - \lambda(\bar{x}_1, \bar{x}_2)]N\}, \quad (10)$$

where

$$G_{rc}(N) \propto (N^\gamma + N^{-2+\alpha}) \exp[\beta(\lambda(\bar{x}_1, \bar{x}_3) - \lambda_0)N], \quad (11)$$

and

$$G_n(N) = NF_n(\bar{n}_1, \bar{n}_3, N). \quad (12)$$

In order to explore the phase behavior of the system we will use the simulation results of Figs. 2 and 3 to obtain the relevant behavior of the functions $\bar{n}_1(N)$, $\bar{n}_3(N)$, $F_n(\bar{n}_1, \bar{n}_3, N)$, \bar{x}_1 , \bar{x}_3 , $\lambda(\bar{x}_1, \bar{x}_3)$ and λ_0 .

The functions $\bar{n}_1(N), \bar{n}_3(N)$ are approximated using the simplest functional forms suggested by the simulation results of Fig. 3 in the limit of large N : $\bar{n}_1(N) \approx c_1 N^\eta$ and $\bar{n}_3(N) \approx c_3 N$, where $0 < \eta < 1$ and c_1, c_3 (both > 0) are constants. In what follows the precise values of c_1, c_3 and η are irrelevant [17]. In the appendix we study the more general case where c_1 and c_3 are functions of ρ and show that the main result of this section does not change. As a consequence, \bar{x}_1, \bar{x}_3 are approximated by $\bar{x}_1 \approx 0$ and $\bar{x}_3 \approx c_3$.

The sublinear correction to the free energy of networks, $-\ln VF_n(N, \bar{n}_1, \bar{n}_3)$, has an entropic and an energetic contribution. The internal energy of a network can be approximated (in a similar way to what has been done in [8,9]) by $E_n(N) = -N\epsilon_0 + \epsilon_1 \bar{n}_1(N) + \epsilon_3 \bar{n}_3(N)$, where ϵ_0 is a ‘‘bond’’ energy (i.e., the internal energy per particle of an infinite chain or ring), and ϵ_1 and ϵ_3 are, respectively, the energy costs of an end and of a junction. Using the approximations adopted for \bar{n}_1, \bar{n}_3 , we obtain $E_n(N) = (-\epsilon_0 + \epsilon_3 c_3)N + \epsilon_1 c_1 N^\eta$. The first term of this sum is linear in N and will contribute to the free energy per particle of an infinite network [i.e., to $\lambda(0, c_3)$]. Therefore, $F_n(N, \bar{n}_1, \bar{n}_3)$ is approximated by

$$F_n(N, \bar{n}_1, \bar{n}_3) = F_S(N) \exp(-\beta \epsilon_1 c_1 N^\eta), \quad (13)$$

where $\beta^{-1} \ln VF_S(N)$ is the excess entropy of a finite N -network ($F_S(N)$ expected to scale with some power of N [16]).

Using these approximations Eqs. (10), (11), and (12) become, respectively

$$\rho^* = \sum_{N=1}^{N_p} [G_{rc}(N) + G_n(N)] \times \exp[\beta[\mu(N_p, \rho^*) - \lambda(0, c_3)]N], \quad (14)$$

$$G_{rc}(N) \propto (N^\gamma + N^{-2+\alpha}) \exp[\beta(\lambda(0, c_3) - \lambda_0)N], \quad (15)$$

$$G_n(N) = NF_S(N) \exp(-\beta \epsilon_1 c_1 N^\eta). \quad (16)$$

The inset of Fig. 2 shows that, for large N , the slope of $\ln \phi_n(N)$ is negative and increases with increasing ρ^* . Since this slope is, from (8), $\beta[\mu(N_p, \rho^*) - \lambda(0, c_3)]$, we conclude that $\mu(N_p, \rho^*)$ is approaching $\lambda(0, c_3)$ as ρ^* increases. Moreover, the simulations at densities $\rho^* = 0.15$ and 0.2 show a size distribution of networks with a positive slope and a peak close to $N = 5000$, which means that for these values of ρ^* one already has $\mu(N_p, \rho^*) > \lambda(0, c_3)$. According to the theory presented in Sec. III, this behavior of $\mu(N_p, \rho^*)$ [given implicitly by Eq. (14)] corresponds to a phase transition if $\rho_t \equiv \sum_{N=1}^{\infty} [G_{rc}(N) + G_n(N)]$ converges.

The simulation results of Fig. 2 show that the slope of $\ln \phi_c(N)$ is smaller than that of $\ln \phi_n(N)$. Since, $\ln \phi_n(N) \approx [\mu(N_p, \rho^*) - \lambda(0, c_3)]N$ and $\ln \phi_c(N) \approx (\mu(N_p, \rho^*) - \lambda_0)N$, $\lambda(0, c_3) - \lambda_0$ is the difference between the slope of $\ln \phi_c(N)$ and that of $\ln \phi_n(N)$. Therefore, $(\lambda(0, c_3) - \lambda_0) < 0$ and $\sum_{N=1}^{\infty} G_{rc}(N)$, with G_{rc} given by (15), converges. Verification of the convergence of $\sum_{N=1}^{\infty} G_n(N)$ is straightforward since $G_n(N)$, given by Eq. (16), is a product of a power of N and an exponential of N^η with $0 < \eta < 1$.

Then, ρ_t converges and, at this density (in the thermodynamic limit, at the given m^*), the system exhibits a transition to a phase where a finite fraction of particles belongs to a macroscopic cluster.

The existence of the transition is related to the properties of the clusters responsible for the convergence of ρ_t . Since the internal energy per particle of the infinite network ($-\epsilon_0 + \epsilon_3 c_3$) is larger than that of the infinite chain ($-\epsilon_0$), $(\lambda(0, c_3) - \lambda_0) < 0$ implies that the entropy per particle of the infinite network is larger than that of the infinite chain. In other words, the difference between the entropies must balance the increase in energy due to the junctions. On the other hand, the increase in the number of ends stabilizes the infinite network, since $0 < \eta < 1$. Thus, the transition corresponds to the emergence of a phase with a large configurational entropy, that balances the loss of translational entropy and the increase of the internal energy.

Using Eq. (14) we find that, in the thermodynamic limit, $\lim_{\rho \rightarrow \rho_t} \left(\frac{\partial \mu}{\partial \rho} \right)_{m^*}$ is positive, and conclude that the transition is discontinuous at $m^* = 2.75$ [18]. A second order phase transition occurs when the second moment of the distribution $\phi(N)$ diverges at ρ_t , as in percolation or Bose–Einstein condensation.

V. CONCLUSIONS

Analysis of extensive MC simulations combined with a theory that includes nonlinear clusters hint at the possibility of the existence of a phase transition of the low density quasi 2D DHS fluid. This conclusion relies on several approximations. As a detailed knowledge of the distribution of networks of different topologies is not available from simulations we approximated it by the distribution of mean fractions of ends and junctions. We further assumed that the scaling with N of these distributions, measured in the simulations up to $N \approx 600$, holds for infinitely large cluster sizes. With these assumptions we have shown that the phase transition is driven by the formation of a macroscopic network, with a large configurational entropy that overcomes the cost in internal energy and the loss of translational entropy of the phase with high connectivity. Whether a similar transition is present in 3D DHS cannot be answered at present since detailed information on the cluster distributions in three dimensional is not available.

Recently, the thermodynamics of a self-assembling system of chains and networks (with no rings and no attractive interactions between clusters) was studied, at the mean-field level, and a phase transition has been predicted [10]. The approximations used in that work for the distributions of chains and networks hinder a quantitative comparison with the results of this paper. Nevertheless, the mechanism, driving the transition, is the same in both approaches.

The full phase diagram of the DHS at low densities may be studied by generalizing the methods described in this paper. However, this entropy driven transition may be preempted by the stabilization of other condensed phases (ordered or not) that are not considered in this framework. This is unlikely to occur at the low densities of the simulations

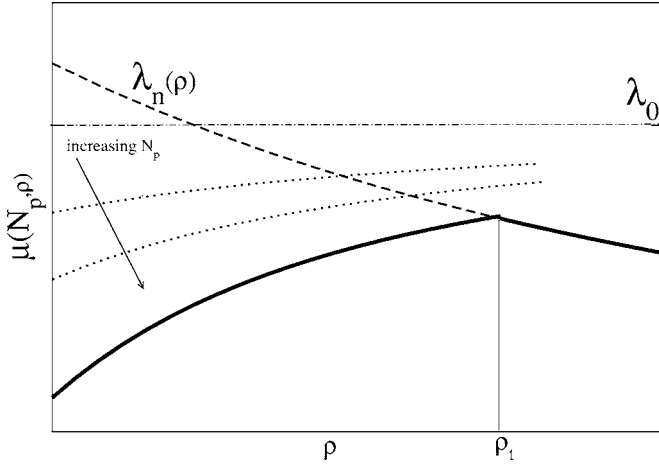


FIG. 5. Generalization of Fig. 4 for the free energy per particle of an infinite network that depends on density. Dotted lines: $\mu(N_p, \rho)$ for finite N_p as given by Eq. (A1). Full line: $\mu(\rho) \equiv \lim_{N_p \rightarrow \infty} \mu(N_p, \rho)$, when $\rho_t \equiv \sum_{N=1}^{\infty} (G_{rc} + G_n)$ [see Eqs. (A2) and (A3)] is finite. Dashed line: free energy per particle of an infinite network, $\lambda_n(\rho)$. Dashed dotted line: free energy per particle of infinite chains and rings, λ_0 .

considered here but may prevent the critical point from being observed.

ACKNOWLEDGMENTS

We acknowledge D. Levesque and P. I. C. Teixeira for a critical reading of this manuscript and for their valuable suggestions.

APPENDIX

In Sec. IV we approximated $\bar{n}_3(N) = c_3 N$ and $\bar{n}_1(N) = c_1 N^\eta$ inspired by the simulation results of Fig. 3. By assuming that c_1 and c_3 are constants, the slight dependence on ρ^* [especially of $\bar{n}_3(N)$] depicted in Fig. 3 has been neglected. In this appendix we show that the conclusion of Sec. IV (the suggestion of the presence of a phase transition) does not change if c_3 and c_1 depend on ρ^* as shown by the simulations.

Let us consider that $\bar{n}_3(N) = c_3(\rho^*)N$ and $\bar{n}_1(N) = c_1(\rho^*)N^\eta$. Then $\lambda(\bar{x}_1, \bar{x}_3)$ becomes $\lambda[0, c_3(\rho^*)] \equiv \lambda_n(\rho^*)$, i.e., the free energy per particle of an infinite typical network at density ρ^* becomes dependent on density. Using these forms for $\bar{n}_3(N) = c_3(\rho^*)N$ and $\bar{n}_1(N) = c_1(\rho^*)N^\eta$ Eqs. (14), (15), and (16) become

$$\rho^* = \sum_{N=1}^{N_p} [G_{rc}(N, \rho^*) + G_n(N, \rho^*)] \exp\{\beta[\mu(N_p, \rho^*) - \lambda_n(\rho^*)]N\}, \quad (\text{A1})$$

$$G_{rc}(N, \rho^*) \propto (N^\gamma + N^{-2+\alpha}) \exp[\beta(\lambda_n(\rho^*) - \lambda_0)N], \quad (\text{A2})$$

$$G_n(N, \rho^*) = NF_S(N) \exp(-\beta \epsilon_1 c_1(\rho^*) N^\eta). \quad (\text{A3})$$

We will start by defining $s_n(\rho^*)$ and $s_c(\rho^*)$ as the slopes, at large N of $\ln \phi_n(N)$ and $\ln \phi_c(N)$, respectively

$$s_n(\rho^*) \simeq \mu(N_p, \rho^*) - \lambda_n(\rho^*), \quad (\text{A4})$$

$$s_c(\rho^*) \simeq \mu(N_p, \rho^*) - \lambda_0. \quad (\text{A5})$$

The simulation results of Fig. 2 show that

$$s_n > s_c \Rightarrow \lambda_n(\rho^*) < \lambda_0, \quad (\text{A6})$$

$$\frac{\partial(s_n - s_c)}{\partial \rho} > 0 \Rightarrow \frac{\partial \lambda_n}{\partial \rho} < 0. \quad (\text{A7})$$

On the other hand, the results of Fig. 3 suggest that $\frac{\partial c_1}{\partial \rho} > 0$ [17].

One can still show that there exists a finite density transition, ρ_t , which is the solution of the equation $\rho^* = F(\rho^*)$ with

$$F(\rho^*) = \sum_{N=1}^{\infty} [G_{rc}(N, \rho^*) + G_n(N, \rho^*)]. \quad (\text{A8})$$

Since $\frac{\partial \lambda_n}{\partial \rho} < 0$ and $\frac{\partial c_1}{\partial \rho} > 0$, $F(\rho)$ is a decreasing function of ρ and one expects that $\lim_{\rho \rightarrow 0} \lambda_n(\rho) = \infty$. Therefore, the function $F(\rho)$ crosses the function ρ and a finite value for ρ_t is obtained. In order to show that the existence of a finite ρ_t implies the presence of a phase transition, we generalize the argument given in Sec. III. For every $\rho < \rho_t$ it is always possible to find a finite value of N_p such that $\mu(N_p, \rho) = \lambda_n(\rho)$. This value of N_p increases when ρ approaches ρ_t so that $\mu(\rho) \equiv \lim_{N_p \rightarrow \infty} \mu(N_p, \rho) < \lambda_n(\rho)$ and $\mu(\rho_t) = \lambda_n(\rho_t)$. On the other hand, for every $\rho > \rho_t$ and every (finite) N_p one has to have $\mu(N_p, \rho) > \lambda_n(\rho)$. At the same time, for every fixed $\rho > \rho_t$ an increase in N_p implies a decrease in $\mu(N_p, \rho)$. As a consequence, when $\rho > \rho_t$, $\mu(\rho) \equiv \lim_{N_p \rightarrow \infty} \mu(N_p, \rho) = \lambda_n(\rho)$. Therefore, if ρ_t is finite, $\mu(\rho)$ converges nonuniformly to the function: $\mu(N_p \equiv \infty, \rho)$ [given through Eq. (5)] if $\rho < \rho_t$; and $\lambda_n(\rho)$ if $\rho \geq \rho_t$. Then, for finite ρ_t , $\mu(\rho)$ is singular at $\rho = \rho_t$, signaling a phase transition at this density. Figure 5 depicts a graphical representation of the functions $\lambda_n(\rho)$, $\mu(N_p, \rho)$ and $\mu(\rho)$ that may help to clarify the previous arguments.

- [1] P. J. Camp, J. C. Shelley, and G. N. Patey, Phys. Rev. Lett. **84**, 115 (2000).
 [2] J. J. Weis and D. Levesque, Phys. Rev. Lett. **71**, 2729 (1993); M. E. van Leeuwen and B. Smit, *ibid.* **71**, 3991 (1993).
 [3] K. Van Workum and J. F. Douglas, Phys. Rev. E **71**, 031502

(2005).

- [4] R. van Roij, Phys. Rev. Lett. **76**, 3348 (1996).
 [5] R. P. Sear, Phys. Rev. Lett. **76**, 2310 (1996).
 [6] J. M. Tavares, J. J. Weis, and M. M. Telo da Gama, Phys. Rev. E **59**, 4388 (1999).

- [7] P. I. C. Teixeira, J. M. Tavares, and M. M. Telo da Gama, *J. Phys.: Condens. Matter* **12**, R411 (2000).
- [8] J. M. Tavares, J. J. Weis, and M. M. Telo da Gama, *Phys. Rev. E* **65**, 061201 (2002).
- [9] T. Tlusty and S. A. Safran, *Science* **290**, 1328 (2000).
- [10] A. G. Zilman and S. A. Safran, *Phys. Rev. E* **66**, 051107 (2002).
- [11] J. P. Wittmer, P. van der Schoot, A. Milchev, and J. L. Barrat, *J. Chem. Phys.* **113**, 6992 (2000).
- [12] V. F. Putes, K. M. Krishnan, and A. P. Alivisatos, *Science* **291**, 2115 (2001); K. Butter, P. H. H. Bomans, P. M. Frederik, G. J. Vroege, and A. P. Philipse, *Nat. Mater.* **2**, 88 (2003); M. Klokkenburg, C. Vonc, E. M. Claesson, J. D. Meeldijk, D. H. Ern e, and A. P. Philipse, *J. Am. Chem. Soc.* **126**, 16706 (2004).
- [13] C. Holm and J. J. Weis, *Curr. Opin. Colloid Interface Sci.* **10**, 133 (2005).
- [14] J. A. Cuesta and R. P. Sear, *Phys. Rev. E* **65**, 031406 (2002); R. P. Sear and J. A. Cuesta, *Europhys. Lett.* **55**, 451 (2001).
- [15] C. T. Gao, X. C. Zeng, and W. Wang, *J. Chem. Phys.* **106**, 3311 (1997).
- [16] J. des Cloizeaux and G. Jannink, *Les Polymères en Solution* (Les Éditions de Physique, Les Ulis, 1987).
- [17] The scattering of the data prevents a fine determination of c_3 , c_1 , η and of the exponent of $\bar{n}_3(N)$ (that we approximated by 1). Nevertheless, if the data of all densities are fitted to a single power law one obtains: $\bar{n}_1(N) \approx 0.086N^{0.63 \pm 0.01}$ (for $50 \leq N \leq 600$) and $\bar{n}_3(N) \approx 0.056N^{0.91 \pm 0.04}$ (for $150 \leq N \leq 600$). If the data of $\bar{n}_1(N)/N$ of each density are fitted to a power law, increasing values of c_1 with ρ^* are obtained.
- [18] In a second order (or continuous) phase transition, one has $\left(\frac{\partial^2 f}{\partial \rho^2}\right)_{m^*} \equiv \left(\frac{\partial \mu}{\partial \rho}\right)_{m^*} = 0$.